Continental Shelf Research 30 (2010) 1772–1782

Contents lists available at ScienceDirect

Continental Shelf Research

journal homepage: www.elsevier.com/locate/csr

Research papers

Multi-beam backscatter measurements used to infer seabed habitats

R.J. Kloser [a,*], J.D. Penrose [b], A.J. Butler [a]

[a] CSIRO Wealth from Oceans, G.P.O. Box 1538, Hobart, Tasmania 7001, Australia
[b] CURTIN University of Technology, Australia

ARTICLE INFO

Article history:
Received 14 February 2010
Received in revised form
5 August 2010
Accepted 6 August 2010
Available online 17 August 2010

Keywords:
Australia
Biotopes
Epifauna
Backscatter
Video
Multi-beam

ABSTRACT

Backscatter from multi-beam sonar (MBS) was used to discriminate ecologically relevant seabed characteristics based on 62 reference sites sampled with georeferenced video, sediment grab and rock dredge between 50 and 500 m water depth. A simple biotope characteristic of soft (unconsolidated) and hard (consolidated) was used to compare the acoustic backscatter data with the data on mega-epifauna and substrate type obtained from video and physical sampling. Substrate type of homogeneous reference sites was predicted by matching the backscatter incidence angle profile (0–70°) to that of a seabed scattering model. Referencing the seabed backscatter to a consistent incidence angle (40°) gave a metric with high spatial resolution (2.4–20 m), which minimised errors of range, incident angle and beam compensation. This simple metric provided a consistent approach to analyse and interpret the data and was strongly correlated with substrate type and faunal functional groups. The high resolution backscatter metric was a closer match to the small spatial scale of seabed patch lengths observed by video (50% <50 m).

1. Introduction

Australia, like many other nations, faces the challenge of managing the resources of an enormous Exclusive Economic Zone. One of the most pressing parts of this challenge is to manage the heavily exploited but poorly understood seabed of the shelf and slope bioregions, between 50 and 1500 m depth (Williams et al., 2009). From an ecological perspective there is a need to understand the biodiversity and biogeography within and between bioregions at a variety of scales (Greene et al., 1999; NOO, 2002; Kloser et al., 2007). A simple first step in this process is to map the spatial scales of the types of terrain and key components of the biotic assemblages to define marine habitat patches (Pickett and White, 1985; Hubbell, 2001; Holyoak et al., 2005; MacArthur and Wilson, 1967). The question addressed in this paper is the extent to which acoustic multi-beam sonar (MBS) methods can be used to detect the nature of habitats, and hence, to make predictions about the fauna of the seabed?

We compare MBS data with optically sensed faunal data and directly sampled seabed data where they have been taken simultaneously and consider whether multi-beam data would aid in predicting the fauna of an area in the absence of visual or direct sampling. The biota of an area can be examined at a variety of spatial scales, the focus can be on large or small organisms (including very small—microscopic or sub-microscopic sizes), and the taxonomic resolution can vary from coarse (phyla, families or simply morphological or functional groups) to fine (species or even subspecies variation). The necessary targeted physical sampling varies in quantity and quality depending on the taxonomic resolution required (Kloser et al., 2007). In this paper we focus on the megafauna (Gage and Tyler, 1996) examined on spatial scales of tens of meter to 1 km. The term "biotope" is used here to refer to a type of seafloor defined by both its physical characteristics (e.g., seabed hardness and roughness, regime of currents, temperature and depth) and the organisms that typically inhabit it.

Acoustic methods of sensing the water column and seabed habitats provide a potential method for developing biotope surrogates when used in conjunction with direct capture and visual sampling methods (Kloser et al., 2001; Anderson et al., 2008). To provide resolution of depth, slope and topography, which improves from that of single-beam methods, MBS is being used (e.g., Kloser et al., 2007; Anderson et al., 2008). A MBS provides detailed bathymetry along the line of the vessel's track with swath widths of 2–5 times water depth and produces detailed acoustic backscatter maps of the seabed. Methods to process and interpret the data from MBS have been evolving. The processing of depth data, removing errors caused by ray bending, platform motion, fish schools, bottom detection method and noise have been developed (e.g., Mitchell, 1996; Calder and Mayer, 2003; Canepa et al., 2003). Advances are also being made in the processing and understanding of seabed backscatter from multi-beam instruments (e.g., de Moustier, 1986; Clarke et al., 1993; Hellequin

* Correspondence to: CSIRO Marine and Atmospheric Research, G.P.O. Box 1538, Hobart, Tasmania 7001, Australia. Tel.: +61 3 62325222.
E-mail address: rudy.kloser@csiro.au (R.J. Kloser).

0278-4343/$ - see front matter Crown Copyright © 2010 Published by Elsevier Ltd. All rights reserved.
doi:10.1016/j.csr.2010.08.004

et al., 2003; Brown and Blondel, 2009). Several commercial software products provide a phenomenological seabed backscatter processing system (e.g., SIMRAD, 1999b; Preston et al., 2003).

Direct biological application of these data, however, are still limited where applications of MBS in shallow waters (<500 m) have concentrated on describing the geology of the seafloor using both the detailed bathymetry and seabed backscatter (e.g., Goff et al., 1999; Todd et al., 1999; Gardner et al., 2003; Dartnell and Gardner, 2004). Recently there has been an effort to use MBS bathymetry and backscatter data for habitat mapping (e.g., Kostylev et al., 2001; Kloser et al., 2002; Edwards et al., 2003; Todd and Greene, 2007). In-situ backscatter calibration of these instruments is not always possible but advances are being made (Foote et al., 2005). For large instruments, relative calibrations are the normal procedure and data from reference sites can be used to calibrate and cross validate the measurements between beams (Hellequin et al., 2003). A consistent methodology for interpretation of seabed backscatter is complicated by the facts that the mean echo and its statistics change with incidence angle for a given seafloor type (roughness and hardness), and that the sampling volume and area resolution of the instrument change with depth and incidence angle. Therefore, several core methods applied separately or in combination are used to analyse the acoustic backscatter based on seabed backscatter models, backscatter statistics and phenomenological characteristics in the data at various spatial scales (Jackson and Richardson, 2007; Brown and Blondel, 2009).

In the frequency range of interest for our depth range, 10–100 kHz, a useful fluid sediment scattering model has been developed over a variety of soft to hard seabed types validated with acoustic measurements (Jackson et al., 1986; Jackson and Briggs, 1992; APL-UW, 1994; Jackson and Richardson, 2007). Measurements on a variety of seabed types have supported the role of the dominant physical scattering mechanisms the model represents over a wide range of incidence angles (Jackson and Briggs, 1992; Williams et al., 2002; Sternlicht and de Moustier, 2003). There are some known limitations of the model and direct inversion of acoustic signals is not possible without setting restricted seabed geoacoustic parameter limits for known seabed types (APL-UW, 1994).

Comparing the acoustic backscatter to the seabed terrain and the associated biota (biotope) requires georeferenced sampling of the seabed and biota at multiple scales (Kloser et al., 2007; Anderson et al., 2008). Adopting the habitat scale terminology of Greene et al. (1999), Kloser et al. (2007) provided an analysis of acoustic terrain sampled in southern Australia at the megahabitat scale (1 m to tens of kilometers) and demonstrated existence of a high degree of patchiness within these acoustic terrain regions. Terrain patchiness at mesohabitat scale (tens of meters to 1 km) is investigated in this paper using reference sites. Reference sites represent regions where there is coincident seabed acoustic backscatter data and either video or physical geological sampling or both. Line transect video at the macrohabitat scale (1 to tens of meters) is assumed to provide an unbiased measure of the large mega-epibenthic faunal communities but has known biases when detecting substrate type and consolidation (Kloser et al., 2007).

Two questions will be investigated in this paper. Firstly, can the MBS metrics be used to determine the nature or type of the seabed terrain (substrate and geomorphology) over a range of depths and between regions? Secondly, can the MBS metrics be used to predict the dominant functional groups of large mega-epibenthic fauna over a range of depths and between regions?

2. Methods

In April 2000, 14 areas, depths 38–600 m off South Eastern Australia (Fig. 1), were surveyed with the RV Southern Surveyor

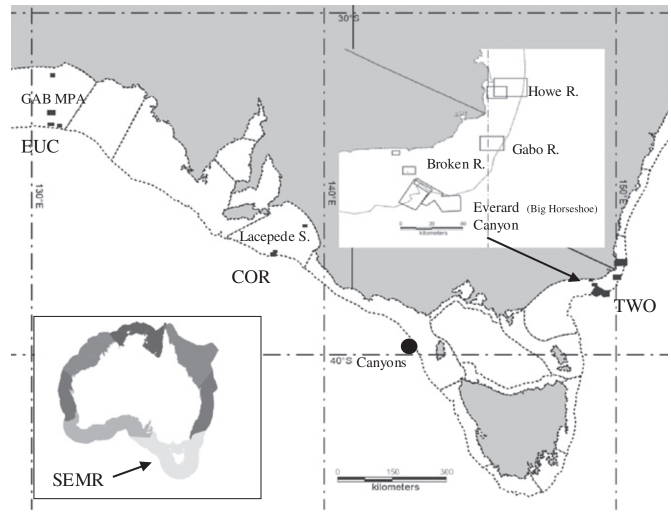

Fig. 1. Large marine domains of Australia (lower left inset highlighting the South East Marine Region (SEMR)) and the survey areas sampled with the EM1002 MBS in the Eucla (EUC), Coorong (COR) and Twofold Shelf (TWO) continental shelf demersal regions (IMCRA Version 4.0 (Commonwealth of Australia, 2006)). The upper right inset highlights the sample areas in the Twofold Shelf region.

using a Simrad EM1002 95 kHz MBS. In these survey areas, 81 reference sites were established with targeted georeferenced biological, physical and optical samplings. The georeferencing was done with a calibrated Sonardyne ultra short base line (USBL) system that for multiple position fixes was estimated to be better than 1% of range, which was typically 2–3 times deep. At the maximum depth of 500 m and range of 1500 m the position error radius was estimated to be less than 41 m for a single position fix and 15 m for multiple position fixes, which is less than 1% of reference site width or length (Kloser et al., 2001b). The reference sites nested within larger 1 km to tens of kilometer terrain patches were selected, based on variability in acoustic backscatter and depth within and between sampled regions, to represent a broad range of contrasting and characteristic seabed types with respect to depth, geomorphology and substrate types (Kloser et al., 2007). In general the terrain was characterised by sandy sediments with low relief limestone/sandstone formations (reefs) on the mid- to outer-shelf and upper slope (Kloser et al., 2001b, 2007).

2.1. Characterising reference sites

2.1.1. Video data

The georeferenced video data represent the highest spatial resolution to determine the seabed terrain and fauna—its image area is 5–7 m^2 and resolution within the image is typically <0.1 m (Kloser et al., 2007). Attributes of the seabed video were scored at 1 s intervals (approx. 0.25 m horizontal distance) in four categories: substrate (6 classes based on Udden–Wentworth scale), geomorphology (7 classes), fauna (10 classes) and faunal abundance (% cover of seabed) (3 classes) (Table 1, Kloser et al., 2007). The video scores of terrain (substrate plus geomorphology scores) were grouped into 4 ecologically important terrain types, namely soft-smooth, soft-rough, hard-smooth and hard-rough. The categories of soft (mud and fine sediment) and hard (granules, pebble, cobble and rock) are hypothesised to relate to the ability of organisms to attach and burrow into the substrate. Soft substrate was also inferred when scoring the video data by the presence of sediment clouds produced by mobile fauna and or when the instrument touched the seabed. Precise sizing of the surficial sediment particle size is limited using video. Hard and soft terrains were further separated into rough and smooth as determined by video data (Table 1). Soft sediment

Table 1
Classes of substrate, geomorphology and fauna used to score benthic terrains and proportions of each for the 62 reference sites (28,492 records); also shown are the inferred terrain types for classifying the reference sites.

%	1. Substrate (S)	Terrain
21	Mud (fine sediments)	Soft
56	Sand (fine sediments)	Soft
11	Coarse granules	Hard
4	Pebble	Hard
1	Cobble	Hard
9	Rock	Hard
%	**2. Geomorphology (G)**	**Terrain**
59	Unrippled	Smooth
3	Current rippled/directed scour	Rough
10	Wave rippled	Rough
4	Highly irregular	Rough
1	Debris flow/rubble banks	Rough
13	Subcrop	Smooth
1	Outcrop	Rough
%	**3. Fauna (F) (dominant fauna community)**	
17	None—no apparent epifauna or infauna	
11	Large sponges—community	
24	Small sponges—community	
0	Mixed sponges, seawhips and ascidians	
2	Crinoids	
0	Octocorals (gold corals/seawhips)	
6	Small encrustors/erect forms (including bryozoans)	
13	Sedentary: e.g., seapens	
1	Mobile: e.g., echinoids/holothurians/asteroids	
26	Distinct infauna bioturbators	
%	**4. Fauna abundance (A)**	
82	Low/sparse ($<10\%$)	
14	Medium/intermediate ($<50\%$)	
4	High/dense ($>50\%$)	

roughness was associated with biological perturbation (bioturbation) or current flow (sand waves) whilst roughness of harder material was associated with consolidated cobble and rock or with cracks and ledges of exposed bedrock/consolidated sediments. Roughness was quantitatively gauged within the 5–7 m^2 viewing area of the video along the line transects using 3 parallel and one crossing laser and knowledge of sizes of captured organisms observed on the video (Barker et al., 2001). Terrain patch length was calculated from the along track video data as outlined in Kloser et al. (2007). Patch lengths represent contiguous scores of a given terrain type with removal of any score bias from oversampling due to image area and scoring rate. Truncated patches at the start and end of video transects are included to retain long patch lengths. Faunal abundance was calculated by estimating the % coverage in the video frame of reference size as low ($<10\%$), medium (10–50%) and high ($>50\%$) (Barker et al., 2001).

2.1.2. Physical seabed samples

Physical sampling of the surficial sediments and rocks was done at 41 reference sites. Surficial sediments were obtained with a Smith–McIntyre grab, which retrieves approximately 0.1 m^3 of sediment per successful deployment. For each grab the sediment (0–20 cm depth) was analysed for grain size (% gravel, sand and mud), total organic carbon content and calcium carbonate content. Wet sieving was carried out using nested 2 mm and 63 μm analytical sieves. Material retained in the 2 mm sieve was *gravel*, that in the 63 μm sieve was *sand* and that collected in the beaker was *mud*. Gravel, sand and mud fractions (mud fraction centrifuged at 4000 rpm) were oven dried at <50 °C and weighed to obtain the percentage of gravel, sand and mud in the sample (Harris et al., 2000). Box core samples were collected to obtain geoacoustic parameters such as porosity, sound speed and density. Rock samples were collected with a rock dredge and analysed by macroscopic description (Folk, 1968; Harris et al., 2000). Sampling positions were merged with geolocation data from the tracking beacon of the USBL used on the samplers and overlaid on MBS backscatter maps. Full details of the sediment sampling are given in Harris et al. (2000). The lithology of rocks within hard reference sites was inferred from visually inspected material retained in targeted rock dredges (Harris et al., 2000).

2.2. Multi-beam sonar

The Simrad EM1002 is a phase interpolated beam-forming MBS with 128 transducer elements forming 111 beams nominally $2^\circ \times 2^\circ$, in a semicircular array, 45 cm radius. This MBS was calibrated following a "patch test" to minimise navigational and motion errors as outlined in the Simrad EM1002 installation manual (SIMRAD, 1999a). A local sound, speed and absorption profile was calculated (Mackenzie, 1981; Francois and Garrison, 1982) based on the temperature and salinity depth profile for each reference site as well as temperature measurements at the transducer face for beam forming calculations. The reference site length along the ship's track was approximately 2.75 times the water depth or at least 50 pings. The seabed depth and the associated seabed backscatter amplitude at the instant of depth determination are calculated for the 111 beams. The system was operated in an equi-distant mode where the angle of incidence of each beam is adjusted to give evenly spaced depth sampling across a nominal flat horizontal seafloor. A reference site contained MBS bathymetric and seabed backscatter data from normal incidence (directly below the vessel) to maximum incidence angle (70° across-track), which for a flat seafloor is a distance of 2.75 times the depth on either side of the track line.

The acoustic depth data were corrected for sound speed errors, outlier identification and vessel-induced motion artefacts following standard procedures using MB system's software (Caress and Chayes, 1995). Anomalous backscatter data were evident when there were inconsistent measured depths and due to aeration under the hull of the vessel. These values were excluded from further computations. The backscatter as calculated by the MBS at the centre of each beam was georeferenced based on the edited bathymetry and corrected for absorption and the estimated ensonified area for the locally derived slope across track (Kloser, 2007). Due to errors in estimating local slopes only deviations greater than 3° were corrected (Kloser, 2007). No corrections for transmit and receive beam pattern errors ($\approx \pm 2$ dB) were done for this data set as they could not be decoupled from the vessel's motion and instrument's beam forming processing. It is estimated that the impact of these errors was minimised to less than ± 1 dB by the analytical techniques described below.

Two simple metrics of the backscatter, ($BS(\theta_i)$ at incidence angle (θ_i), namely its mean and standard deviation expressed in dB were calculated for each reference site and each seabed incidence angle step based on centre of beam backscatter values expressed in linear terms ($bs(\theta_i)$) for n pings within the reference site. Referencing the acoustic backscatter to a consistent reference angle of 40° $BS_{40^\circ}(\theta_i)$ was done by calculating the mean incidence angle profile $\overline{BS(\theta_i)}$ for n pings and subtracting it from the instantaneous backscatter $BS(\theta_i)$, then referencing to the mean backscatter at 40° incidence $\overline{BS(\theta_{40^\circ})}$ where

$$BS_{40^\circ}(\theta_i) = BS(\theta_i) - \overline{BS(\theta_i)} + \overline{BS(\theta_{40^\circ})}.$$

The choice of reference angle needs to maximise the within-site separation and be minimally sensitive to slope correction and absorption errors (Kloser, 2007). Incidence angles between 30° and 50° are suitable and based on the maximum separation of seabed types in the Applied Physics Laboratory at the University of Washington (APL-UW, 1994) seabed scattering model (Fig. 7) and maximum separation of the backscatter standard deviation (Fig. 5b); 40° incidence represents a suitable choice at this frequency and for the seabed types encountered. This method minimised between beam gain errors by subtracting a local mean incidence angle profile (Fig. 9).

2.3. Model backscatter

The APL-UW (1994) seabed scattering model combines the most dominant dimensionless seabed scattering mechanisms of homogeneous sediment volume scattering coefficient $s_v(\theta)$ and surface roughness coefficient $s_s(\theta)$ as a superposition of incoherent scatter to estimate the seabed backscattering strength $S_b(\theta)$, where

$$S_b(\theta) = 10\log_{10}[s_s(\theta)+s_v(\theta)]\mathrm{dB}.$$

Based on the APL-UW (1994) model, the frequency was set to 95 kHz and the MBS data were separated into the model seabed types with geoacoustic properties (Table 2) derived from a synthesis of historic physical seabed samples (Table 3; APL-UW, 1994, table 3.2). The Kolmogorov–Smirnov (KS) test was used to select the best fit between model and measured incidence angle profiles where any between beam gain errors are averaged out in the KS fitting process. To maximise the KS fitting process and match the relative amplitudes of the model and measured backscatter data the model data for all incidence angles were adjusted by −10 dB. This was determined by minimising the KS statistic (mean=0.38, s.d.=0.08, n=75) between 75 measured backscatter sites and the best fit model seabed type.

Table 2
Definition of parameters used in Table 3 for a model of seabed reflectance based on Jackson and Briggs (1992).

Symbol	Definition	Short name
ρ	Ratio of sediment mass density to water mass density	Density ratio
ν	Ratio of sediment sound speed to water sound speed	Sound speed ratio
δ	Ratio of imaginary wave number to real wave number for the sediment	Loss parameter
σ_s	Ratio of sediment volume scattering cross-section to sediment attenuation coefficient	Volume parameter
γ	Exponent of bottom relief spectrum	Spectral exponent
w_2	Strength of bottom relief spectrum (cm^4) at wave number $2\pi/\lambda$ in 1 rad cm^{-1}	Spectral strength

3. Results

3.1. Characterisation of reference sites

3.1.1. Video data

Of the 81 reference sites, 62 contained video information representing 28,492 scored video records within the 50–500 m depth range. A summary of the video score data and its relationship to the backscatter referenced to 40° incidence angle show significant differences between the substrate, geomorphology and faunal scores based on the notched box plot (Fig. 2). Video score data were significantly different at the 5% significance level if their confidence intervals (notches) do not overlap (Fig. 2). In particular as the substrate particle size increases from mud to rock the median backscatter increases non-linearly from −33.5 to −26.5 dB. In particular, coarse granule sediments had higher reflectivity than pebbles and cobble, which may indicate a video scoring bias or that the roughness and consolidation of the seafloor combined for coarse sediments to be more reflective. As the geomorphology changed from unrippled sediment to rocky outcrops the median backscatter increased again non-linearly from −33.5 to −26.2 dB. Of note was the association of some faunal groups to specific backscatter regions; infauna was associated with low backscatter −34.2 dB and the mixed sponge community was associated with high backscatter −27.2 dB (Fig. 2). Infauna was inferred from the video using burrows and holes as clues.

Terrain patch length was highly variable within and between the 62 reference sites and between terrain types. Fine scale patches were evident for all terrain types, where 50% of the patch lengths were less than 58, 120, 18 and 32 m for the soft-smooth, soft-rough, hard-smooth and hard-rough terrains, respectively (Fig. 3). The mean video transect length per reference site was 520 m (s.d.=278) and contained on average 520 video scores assuming an average speed of 1 m s^{-1}. The patchy nature of the terrain at the tens of meters to 1 km scale is evident within the reference sites where 28 sites (45%) contained a proportion of the hard-rough terrain, but 11 of those sites contained less than 19% hard-rough video score. Hard-smooth terrain was observed at 16 sites, none homogeneous, and a high proportion (56%) occurred with less than 19% hard-smooth video score. Soft-rough terrain was only observed at 13 sites (21%), 12 of those had greater than 40% soft-rough video scores with 6 homogeneous ones (100% soft-rough video score). Of the 62 reference sites only 30 were homogeneous, 18 classified as soft-smooth, 6 soft-rough, 0 hard-smooth and 6 hard-rough.

Different faunal groups tended to be more associated with different terrain types (hard, soft, rough or smooth) (Table 4). There are clear regions of association with the hard/soft dimension; hard ground contains >97% of the faunal categories 3–6 whilst the soft ground contains >88% of the faunal categories 7–9 (Table 4). The separation of the faunal categories is not as distinct when splitting by the smooth/rough dimension; two faunal categories are separated at greater than 87% compared with 7 groups separated

Table 3
Characteristics of seabed terrains at 95 kHz and sound speed 1500 m s^{-1} to determine seabed backscatter for Fig. 7 (full listing of 23 seabed types (APL-UW, 1994, table 3.2)).

Sediment name	Bulk grain size Mz (Φ)	Rho ρ	Nu ν	Delta δ	Sigma σ_s	Gamma γ	w_2 w_2 (cm^4)
Rock	–	2.500	2.500	0.01374	0.002	3.25	0.018620
Sandy gravel	−1.0	2.492	1.337	0.01705	0.002	3.25	0.012937
Coarse sand, gravelly sand	0.5	2.231	1.250	0.01638	0.002	3.25	0.006957
Medium sand	1.5	1.845	1.178	0.01624	0.002	3.25	0.004446
Muddy sand	3.0	1.339	1.080	0.01728	0.002	3.25	0.002070
Sandy mud	6.0	1.149	0.987	0.00386	0.001	3.25	0.000518

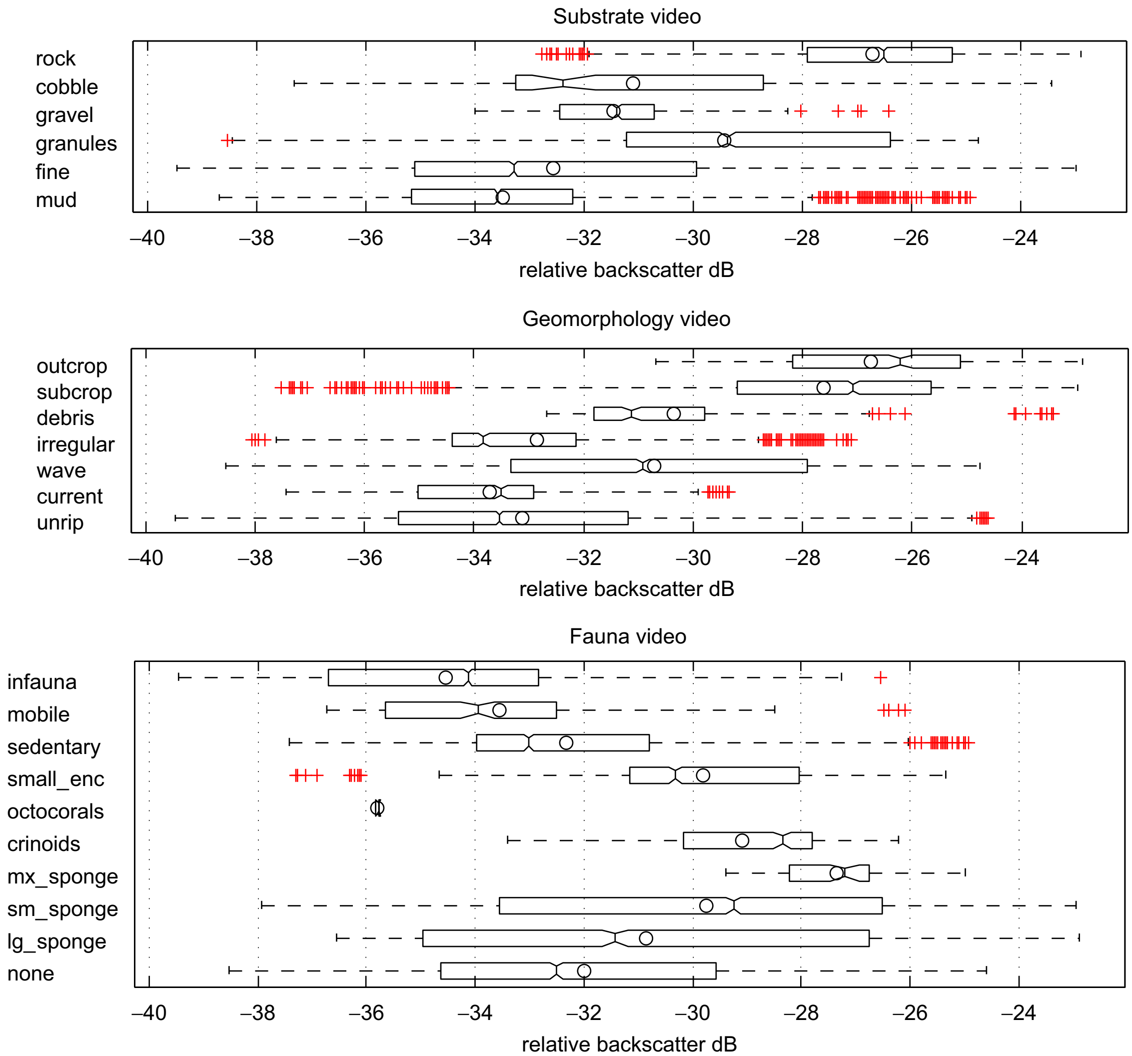

Fig. 2. Summary of the relative acoustic backscatter within reference sites referenced to 40° incidence angle, related to categorised video score data (28,492 records) from 62 reference sites for (a) substrate, (b) geomorphology and (c) fauna. Details of class names and proportions in Table 4. Notch box plot shows the median (bar), mean (circle) and interquartile (25–75%) range and outliers (plus sign) being 1.5 times this range where notches that do not overlap between samples have different medians at the 5% significance level.

on the soft/hard dimension. The small encrustors group (faunal group 6) is strongly (94%) associated with rough terrain whilst sedentary fauna (faunal group 7) are strongly (96%) associated with smooth terrain (Table 4). The abundance (% cover) of the faunal groups on the sea floor changed depending on the terrain type and the faunal group. Faunal group presence varied with terrain type and also the abundance (% cover) varied within and between terrain types. Significantly, higher cover (> 10% of area) of small and large sponge communities (faunal groups 1 and 2) occurs as the terrain gets rougher and harder. When the cover exceeds 50% of the viewing area the sponge communities are only found on hard terrain. Likewise the small encrustor community (faunal group 6) only occurred with high cover on the hard-rough terrain.

Simple separation of soft and hard or smooth and rough terrain types shows that distinct faunal group preferences are evident and prediction (with a high probability) of distributions of faunal groups to terrain types is possible. This relationship is not unique and predictions are not certain, but there are clear and highly significant (greater than 80%) relationships. When percentage cover of organisms is included this relationship strengthens.

3.1.2. *Physical seabed samples*

Physical sampling of the surficial sediments and rocks was carried out at 41 reference sites. Within the homogeneous sites sediment samples showed that the soft-smooth sites contained 13% ($n=11$, s.d.$=8\%$) mud whereas the soft-rough sites contained 1% mud ($n=5$, s.d.$=2\%$). The hard-rough sediment sites contained a higher gravel content (9%, $n=3$, s.d.$=4\%$), but the result is inconclusive due to the difficulty of sampling hard sites with the sediment grab. Hard-rough surfaces such as boulders and consolidated rock outcrops are difficult to sample with a sediment grab and samples may be significantly biased. The lithology of rocks within hard reference sites was inferred from visually inspected material retained in targeted rock dredges (Harris et al., 2000). Accurately directing rock dredges to obtain material within the reference site boundaries was difficult. At depths ranging from 100 to 200 m the lithology consisted of limestone and sandstone and is inferred as being representative of the acoustic terrain of the hard-rough "deep reef" sites at the 1 to tens of kilometers terrain patch size (Fig. 1). Porosity of the rocks varied with "deep reef" location and was visually classified from low to high due to

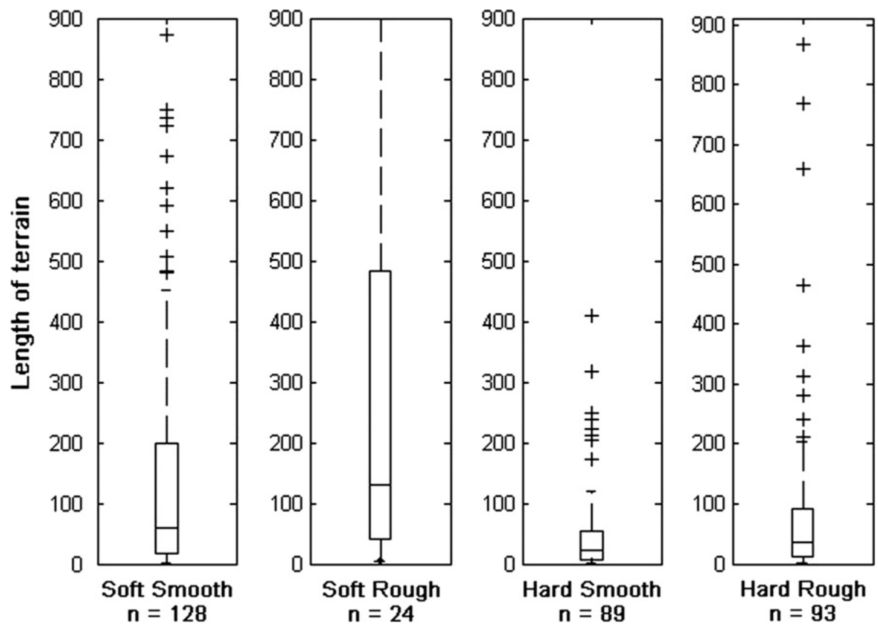

Fig. 3. Box plot of contiguous terrain length (m) frequency for the soft-smooth, soft-rough, hard-smooth and hard-rough terrain types. The box contains the median (bar) and interquartile (25–75%) range and outliers (plus sign) being 1.5 times this range.

Table 4
Proportion (%) of each video scored faunal group in the seabed terrains, soft, hard, smooth and rough, as recorded by the video weighted by terrain type and then faunal type.

Faunal group #scores	**Soft** 24,936	**Hard** 12,440	**Smooth** 23,056	**Rough** 14,320	Description
0	67	33	19	**81**	None—no apparent epifauna or infauna
1	26	74	**84**	16	Large sponges—community
2	30	70	**78**	22	Small sponges—community
3	0	**100**	**85**	15	Mixed sponges, seawhips and ascidians
4	4	**96**	**85**	15	Crinoids
5	0	**100**	**81**	19	Octocorals (gold corals/seawhips)
6	7	**93**	6	**94**	Small encrustors/erect forms (including bryozoans)
7	**100**	0	**96**	4	Sedentary: e.g., seapens
8	**92**	8	32	68	Mobile: e.g., echinoids/holothurians/asteroids
9	**88**	12	40	60	Distinct infauna bioturbators

the inclusion of biological material (Harris et al., 2000; Kloser et al., 2007). These hard platforms were a mosaic of seabed terrains, where the hard-rough portion could be as low as 6% or as high as 99% within the reference site based on video transect scoring. In general as the porosity of the rock increased the backscatter decreased, but this was difficult to quantify due to the fine scale terrain patchiness of the sites.

3.2. MBS backscatter

Fig. 4 shows the seabed backscatter as a function of incidence angle corrected for local slope on a flat seafloor for a homogeneous soft-smooth and a hard-rough reference site. At normal incidence (0°) there is high backscatter for both the terrain types. As the incidence angle increases the soft-smooth terrain backscatter decreases at a faster rate than at the hard-rough terrain site. At 11° incidence it is possible to separate the backscatter of the two seabed types (greater than 50% of the inter-ping variation) using the underlying box plot. The backscatter separation between the two terrains increases with incidence angle to a maximum of 13 dB at 68°. High variation between pings (s.d. 5 dB) is observed near normal incidence and decreases to ≈ 1 dB as the beam angle increases. The variability of backscatter with incidence angle is generally smaller for the soft-smooth terrain. Of note is the correlation (within one or two adjacent incident angle groups) of medians between the two terrain profiles (Fig. 4). These common variations between two very different seabed types indicate a possible instrument calibration variation between beams of approximately ± 2 dB (Figs. 4 and 5). This consistent variation when the vessel has minimal roll between beams was also observed in the average of 11 soft-smooth sites and 15 hard-rough sites (Fig. 5). There is a clear separation (>5 dB at incidence angles $>16^\circ$) between soft-smooth and hard-rough sites using the relationship between backscatter and incidence angle (Fig. 5a). The relative seabed backscatter separation of the profiles decreases from 5 to 0 dB for incident angles 16–0°. Similarly, the standard deviations of backscatter for the mean soft-smooth and hard-rough sites are separated by 0.5–1 dB for incident angles greater than 16° (Fig. 5b). The variation of standard deviation between sites is very low (0.25 dB interquartile range) for the soft-smooth sites and very much higher (0.5–1 dB interquartile range) for the hard-rough sites (Fig. 5b). At incident angles less than 16° the standard deviation of backscatter has overlapping interquartile ranges (Fig. 5b).

Backscatter data from soft-smooth sites where sediment samples contained $<10\%$ mud fraction were significantly different (separation of box plot for incidence angles greater than 16°) from soft-smooth reference sites having $>10\%$ mud (Fig. 6a). The separation of the mean backscatter interquartile range increases with incidence angle, giving higher discriminatory power between % composition mud sites (Fig. 6a). Therefore, it is possible to further segment soft-smooth sites based on % mud using the mean backscatter. In contrast the standard deviation of backscatter from these soft-smooth sites is similar (overlapping interquartile ranges) for $<10\%$ and $>10\%$ mud sites (Fig. 6b). There is high (5 dB) variation at normal incidence reducing rapidly to 2.5 dB (16°) and then reducing gradually to 1 dB at 70° incidence. Whilst it is possible to differentiate between soft and hard sites using the standard deviation of backscatter (Fig. 5b), it is not possible to use this indicator for discrimination within soft sites.

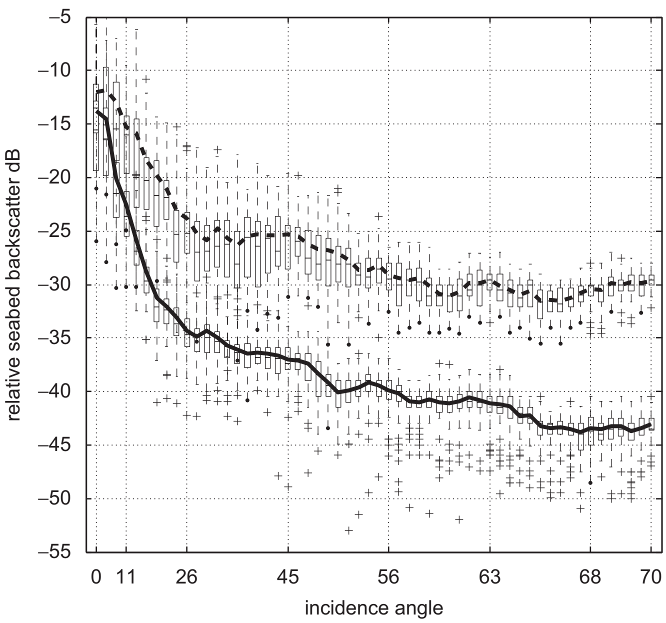

Fig. 4. Variation in relative seabed backscatter (dB) for two reference sites >50 pings on one side of the swath width, soft-smooth (solid) and hard-rough (dashed) for seabed incidence angles of 0–70°. Box plot shows variation of site backscatter dB with median and inter quartile (25–75%) range of dB values; line is the linear mean of backscatter.

3.3. Model comparison of sites and predictions

The backscatter to incidence angle profiles were derived from the APL-UW (1994) seabed scattering model for a set of seabed types of historically measured geoacoustic properties (Fig. 7). There is broad agreement, but there are also significant differences between the APL-UW model and the mean soft-smooth and hard-rough terrain types; these could be influenced by instrument calibration or model accuracy (Fig. 7). At high incidence angles ($>55°$) the model shows a decreasing backscatter whereas the backscatter data for both terrain types increases (Fig. 7). This increase in backscatter could be due to the critical angle that is predicted to occur within this range of incidence angles for sandy sediment sound velocities or elevated between beam gains due to the combined transmitter and receiver beam patterns. In general the hard-rough sites are within the APL-UW (1994) model prediction profiles of medium to coarse sand and the soft-smooth sites within the muddy sand to sandy mud categories.

The predicted seabed grain size in Φ from the APL-UW (1994) model using the best KS fit to the historic geoacoustic seabed properties (Table 3, APL-UW 1994, table 3.2) followed the general trend in measured grain size of the homogeneous soft-smooth sites (Table 5), noting that as the MBS backscatter was not calibrated any comparison is relative. It appears that the absolute sediment grain size is underestimated by the relative MBS

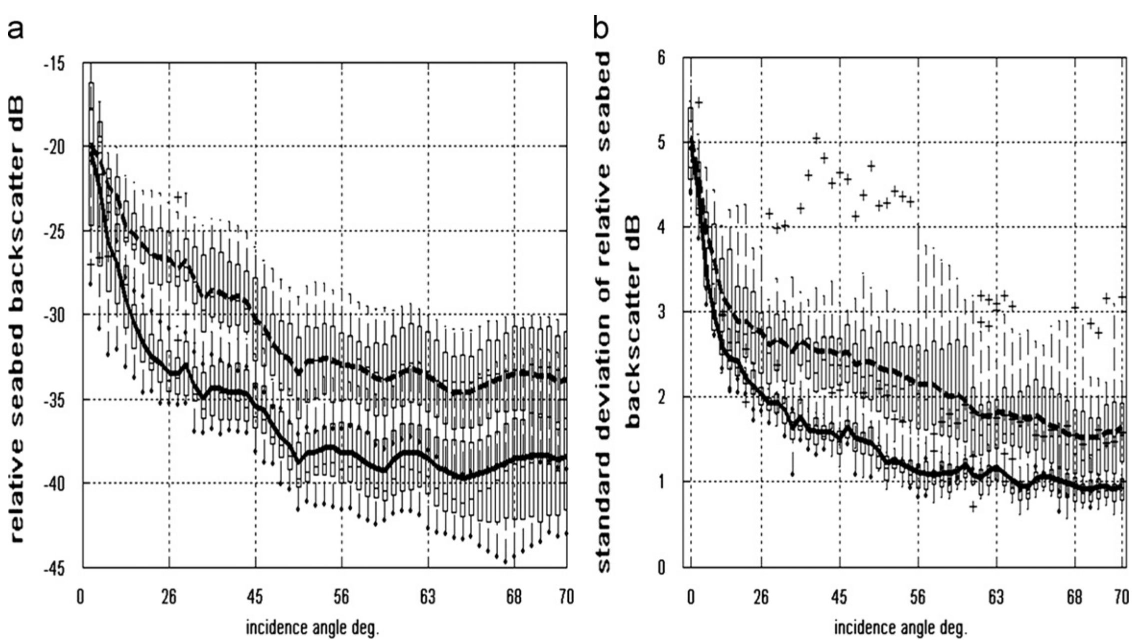

Fig. 5. (a) Variation of relative seabed backscatter between sites for 11 soft-smooth (solid mean) and 15 hard-rough sites (dotted mean) according to seabed incidence angle. Box plot shows variation of site means (dB) with median and inter quartile (25–75%) range; plus signs are outliers. (b) Variation of mean relative standard deviation of backscatter for 11 soft-smooth (dotted mean) and 15 hard-rough sites (solid mean) according to seabed incidence angle where 0° is normal to the seabed. Box plot shows variation of site standard deviation means with median and inter quartile (25–75%) range. Note that backscatter reference angle of 40° occurs at a point of high separation of backscatter standard deviation.

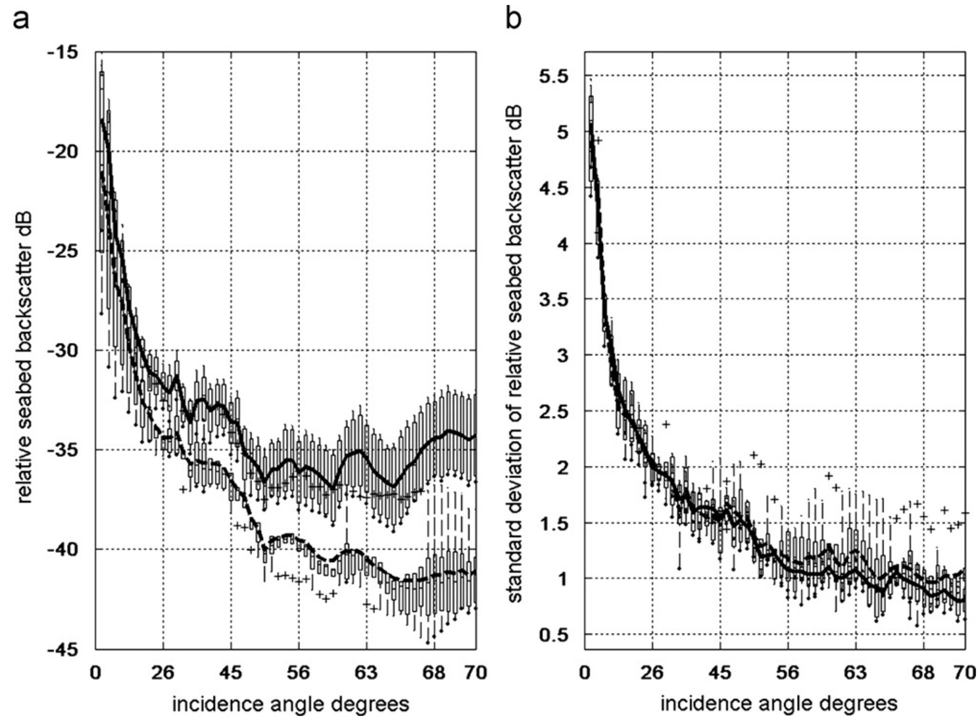

Fig. 6. Variation of backscatter mean (a) and standard deviation (b) for soft-smooth reference sites, 4 with mud composition $<10\%$ (solid mean) and 6 with mud $>10\%$ (dashed mean). Box plot shows variation of site mean and standard deviation means with median and inter quartile (25–75%) range; plus signs are outliers.

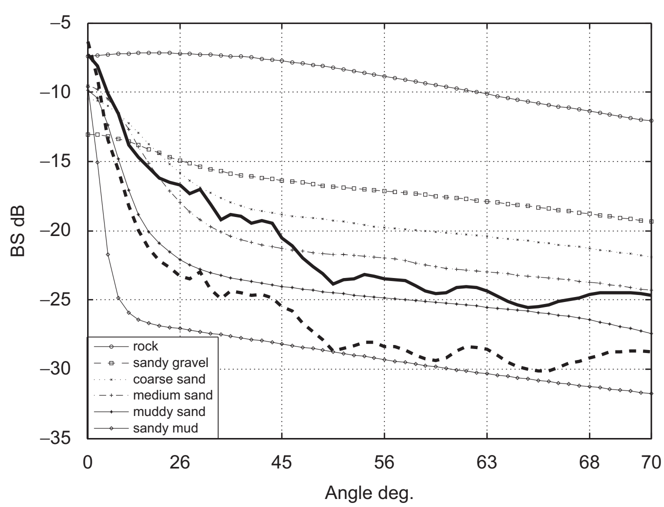

Fig. 7. APL-UW model predictions of typical seabed types ranging from rock to clay terrains assuming geoacoustic properties given in Table 3 at 0–70° incident to the seafloor, and mean backscatter for soft-smooth (dotted) and hard-rough (solid) reference sites adjusted by +10 dB (Fig. 5a). Note that clear separation of model substrate types at 40° reference angle is used in this study where incidence angles between 30° and 50° are suggested as suitable.

backscatter supported by fitted model results suggesting overall calibration was out by 10 dB (Section 2.3). Significantly, as the measured mud fraction increased the model predicted grain size decreased (higher Φ size) ($R^2=0.54$, $n=11$). Higher measured mud compositions in sediment samples were commonly associated with higher model predicted Φ values (i.e. smaller grained sediments Table 5). The predicted mean sediment size of rough-hard sites (mean Φ size$=0.9$, s.d.$=1.7$) was significantly larger than the soft-smooth sites (mean Φ value$=3.8$, s.d.$=1.2$, $n=11$). The difference in the means (2.9 Φ value) was significant at the 0.05 level (Student $t=5.1$, d.f.$=24$). Similarly the relative spectral strength of the seabed is inferred to be rougher for larger sediment sizes using the historic geoacoustic measured seabed properties (Fig. 8).

Removal of the generic incidence angle to backscatter profile by an ensemble ping average and referencing the backscatter to a set incidence angle provides a relative mean backscatter seabed plot that, off normal incidence, could distinguish soft from hard seabed terrain (Fig. 4). Based on the reference site in Fig. 4a 40° referenced incidence angle backscatter profile shows the discrimination achieved (Fig. 9). Using this technique near normal ($<8°$) incidence the overlap of the backscatter distributions reduces the discrimination achieved (Fig. 9). For this site and a MBS that has 111 beams equi-spaced between $\pm 70°$ five beams would on average be pointing between $\pm 8°$. For this site this represents a potential degradation to the ensemble backscatter discrimination of soft and hard of less than 5%. The centre of each beam backscatter data is now at its highest spatial resolution and there are significant relationships between acoustic defined soft and hard terrain (Fig. 9) and video soft and hard terrain and the expected fauna (Table 4, Fig. 2). Based on the 11 soft and 15 hard video classified reference sites (Fig. 5a), 12 hard sites have a mean backscatter of higher than -31 dB and 7 soft sites have a mean backscatter value less than -33.5 dB. Within the amplitude range of -33.5 to -31 dB there were 3 hard sites and 4 soft sites where the seabed has a 36% probability of being hard or 64% being soft (Table 6).

4. Discussion

Australia is responsible for the management of the resources and biodiversity of a very large, deep (50–1500 m) offshore seabed under the United Nations Convention on the Law Of the Sea (UNCLOS). To do this, it is necessary to ascertain the nature, and spatial distribution, of the biological assemblages that occur there. Although this can only be confirmed by direct observation

Table 5
Prediction of relative sediment size (Φ) based on an acoustic scattering model constrained to geoacoustic parameters of typical seabed types (APL94) and minimum Kolmogorov–Smirnov fit to 11 homogeneous soft-smooth terrain reference sites with measured sediment composition (gravel, G; sand, S; mud, M).

Site #	Predicted mean Φ value	KS fit	Measured sediment composition % dry weight			Depth (m)
			M	S	G	
1.05	5.5	0.27	30	67	3	73
13.01	5.5	0.32	19	78	3	144
13.02	5.5	0.32	14	85	1	144
1.06	5	0.39	17	82	1	112
1.07	5	0.34	16	82	2	89
1.08	5	0.21	15	83	2	87
5.07	3	0.13	9	88	3	89
14.03	2.5	0.18	11	86	3	150
1.09	2.5	0.14	5	90	5	90
3.05	1.5	0.21	3	92	5	135
3.05	1	0.14	3	92	5	135

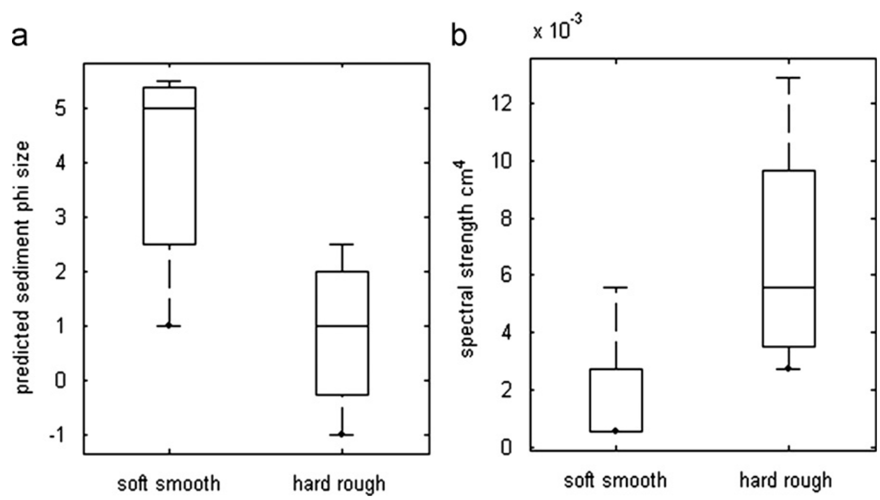

Fig. 8. Model predicted (a) mean sediment grain size (Φ) and (b) spectral strength based on model values (APL-UW, 1994, table 3.2) for the 11 soft smooth and 14 hard-rough reference sites, 50–200 m depth. All values are relative as the MBS backscatter was uncalibrated.

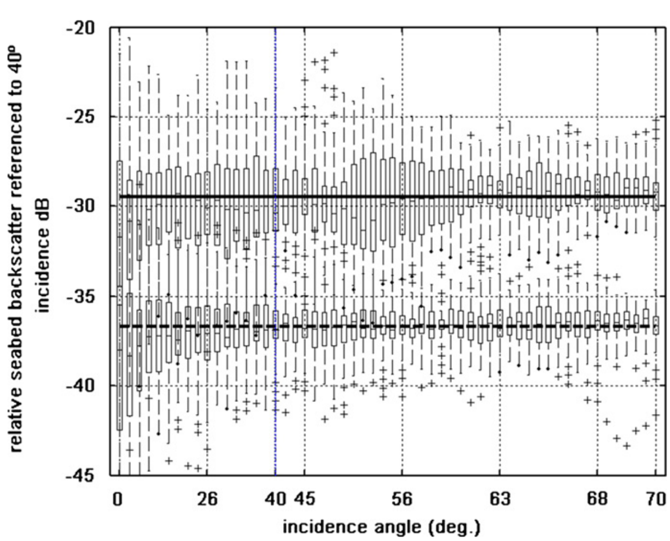

Fig. 9. Comparison of the acoustically hard (solid) and soft (dashed) reference seabed types shown in Fig. 4 referenced to 40° incidence angle. Box plot shows variation of site means (dB) with median and inter quartile (25–75%) range; plus signs are outliers.

and sampling, there is a clear need for a surrogate-based mapping methodology as a first step in predicting the *likely* assemblages over this vast area.

Table 6
Probability % of seabed being classified as hard or soft based on the mean amplitude at 26 reference sites referenced to 40° incidence angle (Fig. 5a).

	Reference site class	
	Hard	Soft
# sites	15	11
Amplitude range (dB) (%)		
> −31	80	0
−33.5 to −31	20	36
< −33.5	0	64

Amongst the possible surrogates, acoustic and optical methods are attractive due to their collective properties: large sampling coverage per unit cost, non-destructive sampling and high spatial resolution (the two methods do, of course, differ in spatial coverage and resolution). The necessary, associated targeted physical sampling varies in quantity and quality depending on the taxonomic resolution required (Kloser et al., 2007). Multi-beam acoustics, in particular, is the only technique that can provide a first-pass coverage of so vast an area in a reasonable time.

The focus of this work, therefore, was to establish a link between acoustic backscatter and faunal functional groups. The acoustic data presented here are not expected to detect the fauna; rather, they give us some information about the substrate. It is recognised, of course, that even if we had a detailed description of the substrate (say, depth, substrate type, aspect, rugosity, particle-size distribution, etc.) this would not specify the associated fauna. It would tell us that a given location is *suitable* for occupancy by – or, likely to be occupied by – a given type of faunal assemblage. But fauna have complex population and community dynamics (Pickett and White, 1985; Holyoak et al., 2005; Kritzer and Sale, 2006) and are affected by factors other than substrate type, so at any point of time, the faunal assemblage may not be what we predict from the substrate. Nevertheless, on that understanding, it is useful to ask whether a classification of terrain types provided by acoustic backscatter is usefully correlated with faunal functional groups.

For this purpose, we used a number of reference sites where MBS data were available together with video observations at scale of tens of meters. The data support the hypothesis that "acoustic terrain types" are correlated with faunal groups (Fig. 2). The most frequently encountered bioturbating infaunal organisms observed from video are associated with soft terrain (88%) and this is associated with mean low backscatter $BS_{40^\circ} = -34.2$ dB. Small encrusting organisms are associated with hard terrain (93%) as observed from video and this is associated with mean higher backscatter $BS_{40^\circ} = -30.3$ dB.

The relative MBS backscatter angular response provides a method of segmenting different substrate types and is supported by visual and physical measurements and a model of seabed scattering. This result builds on previous research in this area (e.g., Williams et al., 2002). Our data show clear mostly consistent beam artefacts due to uncalibrated transmitter and receiver beam patterns that can potentially be removed empirically prior to further processing (Hellequin et al., 2003). The model fitting procedure used here was not sensitive to these consistent beam artefacts as they averaged to zero. Uncertainties with both relative (between beams and within an instrument) and absolute (between instruments) calibration may influence the discrimination of seabed types. Influences of measurement error bias and uncertainty from echo statistics, relative and absolute calibration, sound absorption and aeration due to weather reduce the precision of discrimination. In this case, differences in hard and soft seabed backscatter of >4 dB were measured, which appear to be well within the uncertainties and biases of the instrument and experiments judged to be less than 1–2 dB. The consistent -10 dB difference between model and measured backscatter values highlights the differences in absolute values that can arise when comparing methods.

Fauna and terrain types were patchily distributed. The video data (using the soft, hard, smooth and rough categories) showed that 50% of patch lengths were less than 18–90 m long. In order to understand the distribution of species and species group at this scale, the analysis of the acoustic data needs to resolve better than half this length (9–45 m). Using the backscatter incidence angular response from 0° to 70°, in the 50–500 m depth range investigated here, requires terrain and faunal scales to be of lengths 137–1374 m (2.75 times the water depth, the length of the reference sites). This is much greater than the 18–90 m average terrain patch length observed by video. The resolution of the backscatter data when referencing it to 40° incidence angle is 2.5–20 m across track over the 50–500 m depth range. Using this method we show that for a homogeneous site near normal incidence the error of classification would represent less than 5% of the across swath data. This assumes the EM1002 MBS has $\pm 70^\circ$ emitted incidence angle coverage and the 111 beams are spaced equi-distant across the sea floor. Combining both the angle of incidence response and the referenced backscatter is reported to improve both spatial resolution and terrain discrimination using angular range analysis (Fonseca et al., 2009). To achieve this higher resolution the angular range analysis method requires larger patches of "like type" based on higher resolution normalised backscatter. The actual resolution of acoustic sampling depends on the depth, beam shape, pulse length, signal processing, terrain type and echo statistics. Direct comparison of acoustic metrics with physical and visual samples is complicated by measurement bias or error introduced due to inaccurate geolocation, the different scales of observation, sensor resolution and within patch variability, influencing any inferred fine scale associations. Well described reference sites will assist to determine which acoustic processing method or combination of methods is best for the habitat mapping resolution required, given the terrain and faunal complexity.

It is highly likely that the soft-smooth seabed terrains we examined have suffered cumulative impacts by trawling over many decades, and that we were not sampling "natural" habitats. This would affect the interpretation of the relationship between the terrain and specific faunal groups. Along with natural variation (e.g., succession and community dynamics; Pickett and White, 1985; Holyoak et al., 2005; Kritzer and Sale, 2006), this places a temporal constraint on the interpretation of any acoustic-based classification. As noted above, at best it can tell us what kinds of organisms are likely to occur at a site, but not whether they do, nor their condition. It can contribute to a surrogate-based prediction of the biota at a site but cannot be used for monitoring.

The functional and morphological method of characterizing fauna from the video could, however, be used to monitor changes in seabed due to both natural processes and human activities. As an example, large erect sessile fauna (e.g., sponges) may be removed during bottom-contact fishing whilst smaller sessile organisms remain, and this can be detected using video (Pitcher et al., 1997, 2000; Sainsbury et al., 1997). The scientific reference sites created in this study could provide the start of a system of long-term benthic monitoring sites over a number of bioregions.

This paper focuses on the use of MBS backscatter to characterise the terrain and to infer its likely dominant fauna. We envision this contributing to a surrogate-based, preliminary prediction of the structure and composition of Australia's marine biodiversity, which would be used to guide future detailed sampling, monitoring and management. For example, having knowledge of the proportion of hard and soft terrain available in a given management region would assist the positioning of marine protected areas or fisheries' spatial management planning. To do this on a large scale will require a systematic and sustained protocol for collecting the backscatter data that minimises measurement errors. Specifically within-instrument and between-instrument errors need to be minimised. If the bias and precision of the measurements are less than 1 dB fine scale differences will be observed. If the precision is less than 2 dB it will still be possible to reliably distinguish hard from soft terrain as measured in this study.

5. Conclusion

Based on this work a simple segmentation of acoustic backscatter from MBS, referenced to 40°, can distinguish hard from soft terrain. This has been demonstrated for reference sites at depths of 50–500 m and located in several bioregions. This segmentation of hard and soft terrain could distinguish with high probabilities the faunal functional groups likely to occupy those terrains. This simple but robust method, when associated with appropriate data quality control, would provide a broad scale ecologically relevant metric for substrate type, distinguishing hard from soft terrain. This, in combination with other physical co-variates, could be used to predict the likely faunal community.

Acknowledgements

We would like to acknowledge the contribution of colleagues at CSIRO Marine and Atmospheric Research who assisted in the collection and analysis of the field data. Gordon Keith and Tim Ryan are thanked for the MBS data collection and analysis; Dr Alan Williams, Bruce Barker and Mark Lewis for the video data collection and analysis; Dr Peter Harris and colleagues at GeoScience Australia assisted with collecting and interpreting the geological samples. We thank Dr C. de Moustier for reviews and advice of the acoustic component of the study. Dr N. Bax, Dr J. Keesing and an anonymous reviewer are thanked for reviews of drafts of this paper. Data and funding come from projects supported by the National Oceans Office and CSIRO Marine and Atmospheric Research, the CSIRO Wealth from Oceans National Research Flagship and the CERF Marine Biodiversity Hub.

References

Anderson, J., Holliday, V., Kloser, R.J., Reid, D.G., Simard, Y., 2008. Acoustic seabed classification: current practice and future directions. ICES Journal of Marine Science, 64.

APL-UW, 1994. High frequency ocean environmental acoustic model handbook APL-UW TR 9407. Applied Physics Laboratory Technical Report. University of Washington, Washington, USA.

Barker, B.A.J., Davis, D.L., Smith, G.P., 2001. The calibration of laser-referenced underwater cameras for quantitative assessment of marine resources. Annual Conference of the Marine-Technology-Society, Honolulu, Hi. pp. 1854–1859.

Brown, C.J., Blondel, P., 2009. Developments in the application of multibeam sonar backscatter. Applied Acoustics 70, 1242–1247.

Calder, B.R., Mayer, L.A., 2003. Automatic processing of high-rate, high-density multibeam echosounder data. Geochemistry Geophysics Geosystems, 4.

Canepa, G., Bergem, O., Pace, N.G., 2003. A new algorithm for automatic processing of bathymetric data. IEEE Journal of Oceanic Engineering 28, 62–77.

Caress, D.W., Chayes, D.N., 1995. New software for processing sidescan data from sidescan-capable multibeam sonars. In: Proceedings of the OCEANS 95 MTS/IEEE Conference on Challenges of our Changing Global Environment, San Diego, CA. pp. 997–1000.

Clarke, J.E.H., Mayer, L.A., Mitchell, N.C., Godin, A., Costello, G., 1993. Processing and interpretation of 95 kHz backscatter data from shallow-water multibeam sonars. Oceans 93—Engineering in Harmony with the Ocean, Victoria, Canada. pp. 437–442.

Commonwealth of Australia, 2006. A Guide to the Integrated Marine and Coastal Regionalisation of Australia Version 4.0. Department of the Environment and Heritage, Canberra 16p.

Dartnell, P., Gardner, J.V., 2004. Predicting seafloor facies from multibeam bathymetry and backscatter data. Photogrammetric Engineering and Remote Sensing 70, 1081–1091.

de Moustier, C., 1986. Beyond bathymetry: mapping acoustic backscattering from the deep seafloor with sea beam. Journal of the Acoustical Society of America 79, 316–331.

Edwards, B.D., Dartnell, P., Chezar, H., 2003. Characterizing benthic substrates of Santa Monica Bay with seafloor photography and multibeam sonar imagery. Marine Environmental Research 56, 47–66.

Folk, R.L., 1968. Petrology of Sedimentary Rocks. Hemphill, Austin, Texas.

Fonseca, L., Brown, C.J., Calder, B., Mayer, L., Rzhanov, Y., 2009. Angular range analysis of the seafloor themes from Stanton Banks Ireland: a link between visual interpretation and acoustic signatures. Applied Acoustics 70, 1298–1304.

Foote, K.G., Chu, D.Z., Hammar, T.R., Baldwin, K.C., Mayer, L.A., Hufnagle, L.C., Jech, J.M., 2005. Protocols for calibrating multibeam sonar. The Journal of the Acoustical Society of America 117, 2013–2027.

Francois, R.E., Garrison, G.R., 1982. Sound absorption based on ocean measurements. Part II: boric acid contribution and equation for total absorption. The Journal of the Acoustical Society of America 72, 1879–1890.

Gage, J.D., Tyler, P.A., 1996. Deep-Sea Biology: A Natural History of Organisms at the Deep-Sea Floor. Cambridge University Press, Cambridge.

Gardner, J.V., Dartnell, P., Mayer, L.A., Clarke, J.E.H., 2003. Geomorphology, acoustic backscatter, and processes in Santa Monica Bay from multibeam mapping. Marine Environmental Research 56, 15–46.

Goff, J.A., Swift, D.J.P., Duncan, C.S., Mayer, L.A., Hughes-Clarke, J., 1999. High-resolution swath sonar investigation of sand ridge, dune and ribbon morphology in the offshore environment of the New Jersey margin. Marine Geology 161, 307–337.

Greene, H.G., Yoklavich, M.M., Starr, R.M., O'connell, V.M., Wakefield, W.W., Sullivan, D.E., Mcrea, J.E., Cailliet, G.M., 1999. A classification for deep seafloor habitats. Oceanologica Acta 22, 663–678.

Harris, P., Radke, B., Smith, A., Glen, K., Rollet, N., Exon, N., Passlow, V., 2000. Marine Geological Data Collected During Southern Surveyor Voyage 01/00: Eastern Bass Strait and Great Australian Bight—AGSO Research Cruise Number 224. Australian Geological Survey Organisation.

Hellequin, L., Boucher, J.M., Lurton, X., 2003. Processing of high-frequency multibeam echo sounder data for seafloor characterization. IEEE Journal of Oceanic Engineering 28, 78–89.

Holyoak, M., Liebold, M.A. (Eds.), 2005. Metacommunities: Spatial Dynamics and Ecological Communities. University of Chicago Press, Chicago and London.

Hubbell, S.P., 2001. The Unified Neutral Theory of Biodiversity and Biogeography. Monographs in Population Biology. Princeton University Press, Princeton, NJ.

Jackson, D.R., Briggs, K.B., 1992. High-frequency bottom backscattering: roughness versus sediment volume scattering. The Journal of the Acoustical Society of America 92, 962–977.

Jackson, D.R., Richardson, M.D., 2007. High-Frequency Seafloor Acoustics. Springer, New York.

Jackson, D.R., Winebrenner, D.P., Ishimaru, A., 1986. Application of the composite roughness model to high-frequency bottom backscattering. The Journal of the Acoustical Society of America 79, 1410–1422.

Kloser, R.J., 2007. Seabed biotope characterisation based on acoustic sensing. PhD, Curtin University of Technology, p. 183.

Kloser, R.J., Bax, N.J., Ryan, T., Williams, A., Barker, B.A., 2001. Remote sensing of seabed types in the Australian South East Fishery; development and application of normal incident acoustic techniques and associated 'ground truthing'. Marine and Freshwater Research 52, 475–489.

Kloser, R.J., Keith, G., Ryan, T., Williams, A., Penrose, J.D., 2002. Seabed biotope characterisation in deep water—initial evaluation of single and multi-beam acoustics. In: Stepenowski, A. (Ed.), Proceedings of the 6th European Conference in Underwater Acoustics, Gdansk. pp. 81–88.

Kloser, R.J., Williams, A., Butler, A.J., 2001b. Acoustic, biological and physical data for seabed characterisation. Report to the National Oceans Office, Progress Report 2 of project OP2000-SE02, April 2001. CSIRO Marine Research, Hobart. p. 332.

Kloser, R.J., Williams, A., Butler, A.J., 2007. Exploratory surveys of seabed habitats in Australia's deep ocean using remote sensing—needs and realities. In: Todd, B.J., Greene, H.G. (Eds.), Mapping the Seafloor for Habitat Characterization. Geological Association of Canada, Special Paper 47. pp. 93–110.

Kostylev, V.E., Todd, B.J., Fader, G.B.J., Courtney, R.C., Cameron, G.D.M., Pickrill, R.A., 2001. Benthic habitat mapping on the Scotian Shelf based on multibeam bathymetry, surficial geology and sea floor photographs. Marine Ecology-Progress Series 219, 121–137.

Kritzer, J.P., Sale (Eds.), 2006. Marine Metapopulations. Academic Press, Amsterdam.

MacArthur, R.H., Wilson, E.O., 1967. The Theory of Island Biogeograpghy. University Press, Princeton NJ.

Mackenzie, K.V., 1981. 9-Term equation for sound speed in the oceans. The Journal of the Acoustical Society of America 70, 807–812.

Mitchell, N.C., 1996. Processing and analysis of Simrad multibeam sonar data. Marine Geophysical Researches 18, 729–739.

NOO, 2002. Ecosystems - Nature's diversity: southeast regional marine plan assessment reports. National Oceans office, Hobart, Australia, 214 p.

Pickett, S.T.A. White, P.S., 1985. The Ecology of Natural Disturbance and Patch Dynamics. Academic PressOrlando.

Pitcher, C.R., Burridge, C.Y., Wassenberg, T.J., Poiner, I.R., 1997. The effects of prawn trawl fisheries on GBR seabed habitats. In: The Great Barrier Reef, Science, Use and Management: A National Conference: Proceedings, vol. 1. (Great Barrier Reef Marine Park Authority: Townsville). pp. 107–123.

Pitcher, C.R., Poiner, I.R., Hill, B.J., Burridge, C.Y., 2000. Implications of the effects of trawling on sessile megazoobenthos on a tropical shelf in northeastern Australia. ICES Journal of Marine Science 57, 1359–1368.

Preston, J.M., Parrott, D.R., Collins, W.T., 2003. Sediment classification based on repetitive multibeam bathymetry surveys of an offshore disposal site. In: Proceedings of the MTS/IEEE Conference on Celebrating the Past—Teaming Toward the Future, San Diego, CA. pp. 69–75.

Sainsbury, K.J., Campbell, R., Lindholm, R., Whitelaw, A.W., 1997. Experimental management of an Australian multispecies fishery: examining the possibility of trawl induced habitat modification. In: Pikitch, E.K., Huppert, D.D., Sissenwine, M.P. (Eds.), Global Trends: Fisheries Management. American Fisheries Society, Bethesda, Maryland, pp. 107–112.

SIMRAD, 1999a. Operator Manual EM1002 Multibeam echosounder-160977B. Kongsberg, Horton, Norway.

SIMRAD, 1999b. Triton seafloor classification, instruction manual. In: Kongsberg-Simrad (Ed.). Kongsberg, Horton, Norway.

Sternlicht, D.D., de Moustier, C.P., 2003. Remote sensing of sediment characteristics by optimized echo-envelope matching. The Journal of the Acoustical Society of America 114, 2727–2743.

Todd, B.J., Fader, G.B.J., Courtney, R.C., Pickrill, R.A., 1999. Quaternary geology and surficial sediment processes, Browns Bank, Scotian Shelf, based on multibeam bathymetry. Marine Geology 162, 165–214.

Todd, B.J., Greene, H.G., 2007. Mapping the seafloor for habitat characterisation. Geological Association of Canada special paper 47. p. 519.

Williams, A., Bax, N.J., Kloser, R.J., Althaus, F., Barker, B., Keith, G., 2009. Australia's deep-water reserve network: implications of false homogeneity for classifying abiotic surrogates of biodiversity. ICES Journal of Marine Science 66 (1), 214–224.

Williams, K.L., Jackson, D.R., Thorsos, E.I., Tang, D.J., Briggs, K.B., 2002. Acoustic backscattering experiments in a well characterized sand sediment: data/model comparisons using sediment fluid and Biot models. IEEE Journal of Oceanic Engineering 27, 376–387.